ATTACHMENT-LINE TRANSITION DUE TO ROUGHNESS ON A 76 DEGREE SWEPT CYLINDER AT MACH 1.6

Colin P. Coleman[1]

NASA Ames Research Center, Moffett Field, CA.

Member, AIAA

D. I. A. Poll

College of Aeronautics, Cranfield University, U.K.

Associate Fellow, AIAA

Abstract

Experiments were conducted on a 76° swept cylinder to establish the conditions for the attachment-line transition process with, and without, surface roughness in a low-disturbance ("quiet"), Mach number 1.6 flow. Local flow parameters were estimated from pressure measurements. These were in good agreement with predictions from an Euler code (CFL3D) and a boundary layer code (BL3D). Hot-wires and Schlieren photography were used to determine the state of the boundary layer. It was found that, for a near-adiabatic wall condition and a smooth surface, the attachment-line, boundary-layer remained laminar up to the highest attainable Reynolds number (R-bar of 790). Transition under the influence of trip wires was found to depend on wind-tunnel disturbance levels and the onset conditions have been established. Results suggest that current design practice, which is based upon data from conventional ("noisy") tunnels, may be highly conservative.

Nomenclature

a: speed of sound, $a = \sqrt{\gamma RT}$

---

[1] Research Scientist. M.S. 260-1, NASA Ames Research Center, Moffett Field, CA, 94035-1000

Cp: coefficient of pressure, $Cp = \left(p - p_\infty\right) / 0.5\gamma M_\infty^2 p_\infty$

D diameter of circular cylinder

k diameter of trip wire

M Mach number

p pressure

Q_∞: freestream velocity

r: recovery factor, $r = \left(T_r - T\right)/\left(T_0 - T\right)$

R: gas constant for air, R =287 J/kg K

$\overline{R}$: attachment-line Reynolds number, $\overline{R} = V_e \eta / \nu_e$

$\overline{R}_*$: transformed attachment-line Reynolds number, $\overline{R}_* = V_e \eta_* / \nu_*$

Re_k: trip wire Reynolds number (based on boundary-layer edge conditions), $Re_k = V_e k / \nu_e$

Re_∞: freestream unit Reynolds number, $Re_\infty = Q_\infty / \nu_\infty$

s: distance from trip wire (or cylinder tip if no trip wire present) to hot-wire position, measured along attachment-line

T: temperature

T_*: reference temperature, $T_* = T_e + 0.1\left(T_w - T_e\right) + 0.6\left(T_r - T_e\right)$

U, V, W: velocity components in x, y, z directions, respectively

x: chordwise direction (normal to attachment-line)

y: spanwise direction (along attachment-line)

z: normal direction (normal to cylinder surface)

δ: boundary-layer thickness at $V / V_e = 0.99$

γ: ratio of specific heats of air

η : viscous length scale, $\eta \equiv \left(\frac{\nu_e}{\left(\frac{dU_e}{dx} \right)_{x=0}} \right)^{1/2}$

η_* : transformed viscous length scale, $\eta_* \equiv \left(\frac{\nu_*}{\left(\frac{dU_e}{dx} \right)_{x=0}} \right)^{1/2}$

θ : angle measured from attachment-line in x-direction

ν : kinematic viscosity

Λ_m : sweep angle of cylinder model

Λ_s : shock wave angle

subscripts

0 : stagnation conditions

∞ : freestream conditions

$*$: conditions based on the reference temperature, T_*

A : conditions at the edge of the attachment-line boundary-layer

e : conditions at the edge of the boundary-layer

r : conditions based on the recovery temperature, T_r

w : on surface of cylinder (wall conditions)

Introduction

The incomplete understanding of the attachment line (Figure 1) and crossflow transition processes represents one of the fundamental obstacles to the development of an economically viable, highly efficient, supersonic, laminar flow aircraft. This is especially disturbing since, in the presence of small surface roughness, the flow along an attachment-line may become turbulent at the lowest Reynolds number of all the transition mechanisms that may be active on a swept wing. Should the

attachment-line become turbulent, the flow on the rest of the wing, both upper and lower surfaces, may also become turbulent, leading to higher drag and increased fuel costs.

This unsatisfactory situation can only be resolved by the analysis of data obtained from carefully designed and carefully conducted experiments, where engineering issues and questions of fundamental physics can be addressed at the same time. Experiments conducted on swept cylinders are valuable, since the physics of transition is determined by the boundary-layer characteristics and the appropriate parameters are the local Reynolds number ($\overline{R}$), and the Mach number at the edge of the layer (M_e)[1]. It is possible to generate very large values of $\overline{R}$ on relatively small wind tunnel models and data, which are directly applicable to flight, can be obtained. In an attempt to collapse compressible data to an incompressible form, Poll proposed[2] that a modified Reynolds number ($\overline{R}_*$) be used which evaluates the boundary layer parameters at the reference temperature condition (T_*).

To date, no theoretical model for the stability of a compressible attachment-line flow has been fully validated. The main reason for this is the very limited amount of accurate, experimental data currently available. Although transition has been observed on smooth and tripped configurations and over a wide range of freestream Reynolds numbers and Mach numbers[3-10], there have been no measurements in unstable viscous layers at, or near, an attachment-line in low supersonic Mach number flow. Therefore, experiments[11-12] were conducted to establish the behavior of the attachment-line transition process in a low-disturbance ("quiet"), Mach number 1.6 flow.

Description of Wind Tunnel and Models

Tests were carried out in the Mach 1.6 Quiet Wind Tunnel in the Fluid Mechanics Laboratory (FML) at NASA Ames Research Center. This facility, described in detail in references (11,13-14), was designed to produce laminar flow on the tunnel walls. This produces a novel, low-freestream turbulence and noise level flow for unit Reynolds number ranging from 2.4×10^6/ft to 3.6×10^6/ft. Figure 2 shows the test section pressure fluctuations (p_{rms}/p_{total}) at a location one inch downstream of the nozzle exit. Currently, the consensus view is that a flow is deemed to be "quiet" if the freestream is spatially and temporally uniform with acoustic and convected disturbances (ratio of total pressure rms

to total pressure - p_{rms}/p_{total}) less than 0.1%[13-15]. Since the data are all well below this level and approaching that of the signal noise level, the tunnel is quiet in an acoustic sense. Using a 5 μm tungsten hot wire, the freestream fluctuation value at the centerline of the tunnel was shown to be 0.035%[12].

In order to raise the disturbance level of the test section, ½ inch wide strips of size 80 grit sandpaper (0.025 inch height) were stuck to upper and side walls of the tunnel. The weak shock waves generated by the trips passed in front of the model and did not interfere with the attachment-line, boundary layer. These trips were sufficient to produce turbulent boundary layers on the tunnel walls and these irradiate the test section with acoustic disturbances. Figure 2 shows that tripping the tunnel walls increases the rms pressure disturbance level of the freestream by a factor of eight. This noise was found to be broadband, with no particular frequency being preferred, Figure 3.

The leading edge flow was generated on a circular cylinder swept at 76° to the Mach 1.6 freestream with the apex aligned with the streamwise flow, Figure 4. Two models (identical in external geometry) were used; a pressure model from which local boundary-layer parameters could be estimated and compared with CFD results and a model instrumented with thermocouples for the transition tests. Both cylinders had an external diameter of 1.6 inches and were 16 inches in length. They were supported from the upper wall of the test section by a wedge-shaped spacer, so as to be forward swept in the centerline vertical plane, as shown in Figure 5. This configuration was chosen to prevent the apex touching the floor of the tunnel and contaminating the attachment-line flow with the tunnel wall boundary layer. The configuration was such that the bow shock from the upstream tip reflected from the upper wall and impinged upon the attachment line, thus ending the useful test length of cylinder, at approximately 8 inches from the tip.

One cylinder was made of aluminum 6061-T6 and had a wall thickness of approximately 1/8 inch. The surface was highly polished and finished to better than 1×10^{-5} inches rms. Five T-type thermocouples were evenly placed along the attachment line, from 3.7 inches to 11.7 inches ($2.3 < y/D < 7.3$) from the apex. Flow state in the attachment-line boundary-layer on this model was determined by using a 2.5μm diameter copper plated tungsten hot-wire anemometer. The hot-wire

probe was attached to the cylinder surface using two plastic ties wraps. The height of the wire above the model surface was set at 0.010 inch in the wind-off condition.

In order to estimate the chordwise velocity gradient, which is required in order to obtain $\overline{R}$, the chordwise pressure gradient had to be determined. In previous experiments (with the exception of Yeoh[16]), this information has been obtained from infinite swept conditions or empirical calculations. This was deemed unacceptable for the present study, since accurate values for $\overline{R}$ were required. Pressure tap orifices are known to cast off disturbances, which could influence boundary-layer transition data, and so a second model was used for measurements. This had a series of taps placed along the attachment-line from 3.7 to 7.7 inches ($2.3 < y/D < 4.8$) from the apex, at one inch intervals. At each spanwise location, they extended in the chordwise (normal to the attachment-line) direction from -50° to +50°, in 10° intervals, making a total of 66 pressure measuring points.

Mean Flow CFD Calculations

The CFD code CFL3D[17] was run, in inviscid mode, to calculate the mean flow around the cylinder. This provided the viscous-layer edge conditions, which were then used for boundary layer computations using a simplified version of BL3D[18]. The CFL3D grid used a C-H topology consisting of (222,74,102) points in the (x,y,z) directions, respectively. CFL3D was operated in Euler mode with flux difference splitting. BL3D was run for the adiabatic wall case. The boundary layer grid was specified, in order to calculate attachment-line parameters. It did not extend in the chordwise direction, and consisted of (52,81) points in the (y,z) directions, respectively.

The resulting $\overline{R}$ and $\overline{R}_*$ distributions at two freestream conditions are shown in Figure 6. These correspond to the maximum and minimum values obtainable experimentally in the Mach 1.6 Quiet Wind Tunnel for 1.6 inch diameter models at 76 degree sweep. It should be noted that this arrangement produces an $\overline{R}$ in excess of 700, which is close to the level expected on the proposed HSCT aircraft. Figure 7 show the corresponding viscous length scale, η, and boundary layer thickness δ along the attachment line. Within two diameters' distance from the tip, the boundary layer thickness reaches a near-constant value at all conditions.

Evaluation of $\overline{R}$ From Pressure Measurements

At each spanwise location, the chordwise distribution of velocity is needed and this requires a knowledge of the boundary layer edge temperature and pressure at the attachment line (p_A and T_A, respectively[19-20]). With the instrumentation available, it was not possible to obtain direct measurements of T_A and, therefore, it was necessary to obtain T_A from a knowledge of the local surface static pressure (p_A) and shock angle (Λ_s).

Consider the situation sketched in Figure 4. The streamline that first enters the boundary layer at the point (1) has passed through the bow shock at the point (2). Hence, we may write:

$$\frac{p_A}{p_\infty} = \frac{p_A}{p_{0_1}} \frac{p_{0_1}}{p_{0_\infty}} \frac{p_{0_\infty}}{p_\infty}$$

Incorporating the oblique shock relations, it follows[19] that:

$$\frac{T_A}{T_\infty} = \left[\frac{p_A}{p_\infty}\right]^{\frac{\gamma-1}{\gamma}} \left[\frac{(\gamma-1)M_\infty{}^2 \cos^2\Lambda_s + 2}{(\gamma+1)M_\infty{}^2 \cos^2\Lambda_s}\right] \left[\frac{2\gamma M_\infty{}^2 \cos^2\Lambda_s - (\gamma-1)}{(\gamma+1)}\right]^{\frac{1}{\gamma}}$$

This equation allows the unknown temperature T_A to be obtained from the measured surface static pressure and the shock sweep angle, measured from Schlieren photographs. All other flow parameters at the edge of the attachment-line boundary layer follow immediately[19].

When examining Schlieren photographs, it is necessary to know where the streamline that impacts the attachment line at a given y location, crosses the bow shock wave. In general, this is not known. Therefore, an analysis was undertaken to determine the sensitivity of T_A to the shock angle Λ_s. Now:

$$\left(\frac{p_{0_\infty}}{p_{0_1}}\right)^{\frac{\gamma-1}{\gamma}} = \frac{\left(\frac{T_A}{T_\infty}\right)}{\left(\frac{p_A}{p_\infty}\right)^{\frac{\gamma-1}{\gamma}}}$$

Therefore, for fixed freestream conditions and known p_A, T_A depends upon p_{0_∞} / p_{0_1}. This ratio is plotted in Figure 8 as a function of freestream Mach number and shock angle. For Mach 1.6, p_{0_∞} / p_{0_1} is approximately constant up to a value of Λ_s of 65°. Since Schlieren visualization showed that the bow shock wave was still highly curved near the apex of the cylinder[12] and, since the streamline of interest must pass through the shock close to the apex, Λ_s will be below this value. Consequently, the value of Λ_s has very little effect on the results of this calculation. If the freestream Mach number was higher, the choice of Λ_s would become much more important and some form of flow visualization would be required to establish the exact point at which the streamline of interest crossed the bow shock.

The chordwise velocity was shown by Poll[20] to be given by:

$$U_e = a_A \left\{ \frac{2}{\gamma - 1} \left[1 - \left(\frac{p_e}{p_A} \right)^{\frac{\gamma - 1}{\gamma}} \right] \right\}^{\frac{1}{2}}$$

Although strictly valid for an infinite swept flow, provided that V_∞ does not vary significantly with θ, the relation holds for a finite length model. It was found that by fitting fifth order polynomials to the chordwise velocity distribution, accurate estimates of the velocity gradient term could be obtained[12]. Therefore, fifth order polynomials were fitted to the velocity distributions obtained at each spanwise location using a least squares technique.

Surface Pressure Results

The three parameters of interest, p_{0_∞}, p_∞ and $p_e - p_\infty$, were acquired for freestream unit Reynolds numbers 2.4x10^6/ft to R_{e_∞} =3.4x10^6/ft in 0.2x10^6/ft intervals. They were recorded by the A/D at 50Hz for 80 seconds, giving a total of 4000 samples over three channels, and were averaged to produce mean pressures and a mean value of Cp for each port[12]. As expected, there was no variation in the Cp distribution due to changes in the freestream unit Reynolds number. Figure 9 shows the

complete distribution over the cylinder. The experimentally obtained Cp distribution along the attachment line is compared with the CFD solution in Figure 10. The two are similar and both are approaching the infinite swept value of 0.061 at large y/D. Figure 11 shows the experimentally obtained $\overline{R}$ distribution for freestream unit Reynolds numbers of 2.4×10^6/ft and 3.4×10^6/ft. Compared to the CFD results, the experimental values are higher by about 10%. For the purposes of data reduction, the experimental values have been used.

Surface Temperature Results

Thermocouple response to changes in tunnel free-stream, total temperature was rapid and the model reached thermal equilibrium – approximately adiabatic wall - in a few minutes. The temperature along the attachment line was almost uniform, with the maximum difference between any two thermocouples being of the order 1°F. Based on a wall temperature of 0°F (-17.8 °C) and a stagnation temperature of 20°F (-6.7 °C), the recovery factor for the laminar flow was estimated to be 0.844.

Flow Visualization

Schlieren visualization showed that the bow shock wave was attached at the tip and was curved. The overall shape was in reasonable agreement with the CFL3D solution. At the tip, the shock wave angle was 50° reducing to 43°, whilst the CFL3D solution gave 45° reducing to 40°. Figure 12 shows the reflected bow shock wave hitting the rear of a hot-wire probe at a spanwise distance of 9 inches (y/D=5.6) from the tip. There were very weak Mach waves emanating from various joints of the wind tunnel walls. However, they are located near to the walls, and they do not span the tunnel. None impinged on the transition test surface of the model.

Oil flow visualization was also used to gain an understanding of the overall flow pattern[12]. The line of flow separation was clearly visible at around 90 degrees upstream of the incident shock wave, moving up to 70 degrees downstream of the shock This provided additional evidence that the attachment-line boundary layer was free from external disturbances.

Transition and Trip Wire Results

With the hot-wire probe positioned just in front of the reflected bow shock wave, it was found that, for adiabatic wall condition, the 'clean' (no trip) cylinder had a laminar, attachment line flow up to the highest Reynolds number attainable ($\overline{R}$ approximately 790 at a distance of s/η =3300 from the apex).

Trip wires were then placed on the model. During these tests, the hot-wire was always positioned at 8 inches from the apex, to maximize spanwise test length, and trips (from 0.001 inch to 0.025 inch diameter) were placed at various distances from the tip (from 3.88 inch to 7.5 inch). A weak pressure gradient along the cylinder is evident between the location of the trip wires ($2.4< y/D <4.7$) and the hot-wire (y/D =5.0), Figure 10.

The placement of different trip wires at various distances from the cylinder tip over the Reynolds number range permitted the observation of laminar, intermittent and fully turbulent flows. Turbulent hot-wire signals, with the characteristic power spectrum, were obtained with large trip wires and these differed considerably from the laminar (untripped) signals under the same condition. Focused Schlieren flow visualization of the attachment-line, boundary-layer was also attempted, Figure 13. This provided an estimate of the laminar and turbulent boundary layer thickness of 0.007 inch and 0.025 inch, respectively. The laminar result can be compared with the BL3D solution of 0.009 inch.

During one test, in which a 0.009 inch trip was placed at 6.5 inch from the tip with the hot-wire at 8.0 inch, laminar, intermittent and fully turbulent flows were observed as the Reynolds number was increased, Figure 14. The appearance of turbulent flow was accompanied by a rise in the equilibrium wall temperature and the recovery factor rose from 0.86 to 0.88. An intermittency (first appearance of bursts) of 5% was used as a threshold for the definition of transition onset.

The tripped flow results are shown in Figures 15 and 16. Figure 15 shows that the trip Reynolds number for this Mach number appear to be just below 1900 (note that Re_k is based on boundary layer edge conditions). This result is in agreement with the critical trip Reynolds number of 2000 for a flat plate at a Mach number of 2.0 with an adiabatic wall[21].

Figure 16 displays these results as $\overline{R}$ versus k/η [22]. A transition onset boundary, offset from the previous incompressible results of Poll, is evident. Figure 17 presents the results using the Poll transformed variable $\overline{R}_*$ and k/η_*. The first thing to note is the shift to higher k/η_* of the transition onset boundary. This may be due to the low-disturbance testing environment. Increased wind tunnel disturbance levels in the presence of trips can have a marked effect on the transition process. This has been observed by Creel[4-5]. To test this hypothesis, a simple test was carried out. When the tunnel was 'clean' and a 0.005 inch diameter trip wire was placed on the cylinder at 4 inches from the apex, the recorded signal at y=8 inch was laminar ($\overline{R}$ =790, k/η =2.04). With the tunnel wall boundary layer tripped and the freestream disturbance level increased, (Figure 3), intermittent bursts were observed at the same condition. This suggests that increased levels of tunnel disturbances do reduce the Reynolds numbers for transition to turbulence in the presence of a trip wire.

Summary

A procedure for the estimation of the attachment-line Reynolds number, $\overline{R}$, from surface pressure measurements and Schlieren visualization, has been outlined. Theoretical values of $\overline{R}$ have been shown to be in reasonable agreement with those obtained experimentally. It has been shown that in the low disturbance environment of the Ames quiet tunnel and for near adiabatic wall conditions, the attachment-line boundary layer remains laminar up to the largest obtainable $\overline{R}$ (790 at an s/η of 3300). It has also been shown that attachment-line boundary layer transition in the presence of 2-D trips, is a function of both trip diameter and wind tunnel disturbance level. An approximate transition onset boundary has been established. The present results suggest that current design practice, based on previous results from conventional tunnels, may be excessively conservative.

Acknowledgments

The assistance of Dr. Venkit Iyer (High Technology Corp., Hampton, VA) is greatly appreciated for providing the CFL3D and BL3D computational grids and CFD consultation. Mr. James Heineck (NASA Ames) is also acknowledged for his assistance with the Schlieren photographic technique.

References

[1] Poll, D. I. A., "Transition in the Infinite Swept Attachment Line Boundary Layer", *The Aeronautical Quarterly*, Vol. 30, 1979, pp. 607-629.

[2] Poll, D. I. A., "The Development of Intermittent Turbulence on the Swept Attachment Line Including the Effects of Compressibility", *The Aeronautical Quarterly*, Vol. 34, 1983, pp.1-23.

[3] Arnal, D., Vignau, F. and Juillen, J. C., "Boundary Layer Tripping in Supersonic Flow", *Laminar-Turbulent Transition*, IUTAM Symposium, Toulouse, France, 1989.

[4] Creel, T. R. and Beckwith, I. E., "Effects of Wind-Tunnel Noise on Swept Cylinder Transition at Mach 3.5", AIAA Paper 86-1085, May 1986.

[5] Creel, T. R., Beckwith, I. E. and Chen, F. J., "Transition on Swept Leading Edges at Mach 3.5", *Journal of Aircraft*, Vol. 25, 1987, pp. 710-717.

[6] Da Costa, J. L., de la Chevalerie, D. A. and de Roquefort, T. A., "Leading Edge Transition by Contamination in Hypersonic Flow", AGARD CP-438, 1988.

[7] Holden, M. and Kolly, J., "Attachment Line Transition Studies on Swept Leading Edges at Mach Numbers from 10 to 12", AIAA Paper 95-2279, June 1995.

[8] Murakami, A., Stanewsky, E. and Krogmann, P., "Boundary-Layer Transition on Swept Cylinders at Hypersonic Speeds", *AIAA Journal*, Vol. 34, No. 4, 1996, pp. 649-654.

[9] Skuratov, A. S. and Federov, A. V., "Supersonic Boundary Layer Transition Induced by Roughness on the Attachment Line of a Yawed Cylinder", *Izvestiya Akademii Nauk SSSR, Mekhanika Zhidkosti i Gaza*, Vol. 6, 1990, pp. 28-35.

[10] Benard, E., Gaillard, L. and Alziary de Roquefort, T., "Influence of Roughness on Attachment Line Boundary Layer Transition in Hypersonic Flow", *Experiments in Fluids*, Vol. 22, 1997, pp.286-291.

[11] Coleman, C. P., Poll, D. I. A., Laub, J. A. and Wolf, S. W. D., "Leading Edge Transition on a 76 Degree Swept Cylinder at Mach 1.6", AIAA Paper 96-2082, 27th AIAA Fluid Dynamics Conference, June 17-20, 1996.

[12] Coleman, C. P., "Boundary Layer Transition in the Leading Edge Region of a Swept Cylinder in High Speed Flow", NASA/TM-1998-112224, March 1998.

[13] Wolf, S. W. D., Laub, J. A. and King, L. S., "Flow Characteristics of the NASA-Ames Laminar Flow Supersonic Wind Tunnel for Mach 1.6 Operation", AIAA Paper 94-2502, June 1994.

[14] Wolf, S. W. D. and Laub, J. A., "Low-Disturbance Flow Characteristics of the NASA-Ames Laminar Flow Supersonic Wind Tunnel", AIAA Paper 96-2189, June 1996.

[15] Laufer, J., "Factors Affecting Transition Reynolds Numbers on Models in Supersonic Wind Tunnels", *Journal of Aeronautical Sciences,* Vol. 21, 1954, pp. 497-498.

[16] Yeoh, K. B., "Transition Along the Attachment Line of a Swept Cylinder in Supersonic Flow", M. Sc. Thesis, Cranfield College of Aeronautics, September 1980.

[17] Thomas, J., Krist, S. and Anderson, W., "Navier-Stokes Computations of Vortical Flows", *AIAA Journal*, Vol. 28, No. 2, 1990, pp. 205-212.

[18] Iyer, V., "Three-Dimensional Boundary-Layer Program (BL3D) for Swept Subsonic or Supersonic Wings With Application to Laminar Flow Control", NASA CR 4531, 1993.

[19] Poll, D. I. A., "Boundary Layer Transition by Attachment-Line Contamination in a Compressible Flow with Heat Transfer", Department of Aeronautical Engineering Report 8911, University of Manchester, England, July 1989.

[20] Poll, D. I. A., "3-D Transition to Turbulence by Contamination. Part II - Accurate Determination of the Attachment-Line Chordwise Velocity Gradient", Department of Aeronautical Engineering Report 9311, University of Manchester, England, March 1993.

[21] Gibbings, J. C., "On Boundary Layer Transition Wires", Aeronautical Research Council, CP-462, 1959.

[22] Poll, D. I. A., "Some Aspects of the Flow Near a Swept Attachment Line with Particular Reference to Boundary Layer Transition", Cranfield Institute of Technology, College of Aeronautics Ph.D. Thesis, June 1978.

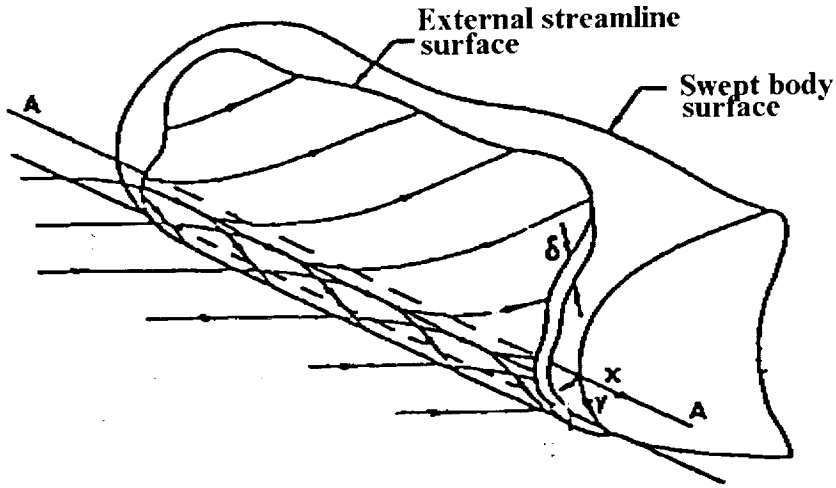

Figure 1. The attachment line (line A-A) boundary layer formed on the swept leading edge of an aircraft wing.

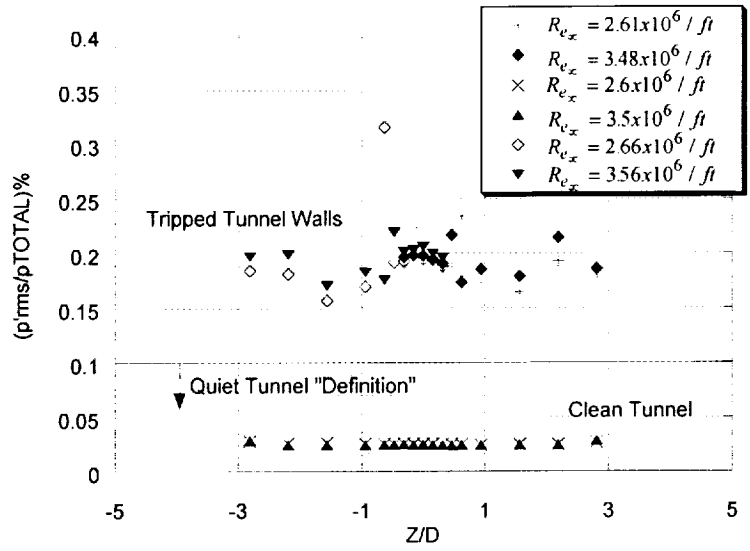

Figure 2. Pressure fluctuations across the center of the test section, 1.0 inch downstream of the nozzle exit with and without tripped tunnel walls. 250 Hz-100 kHz range.

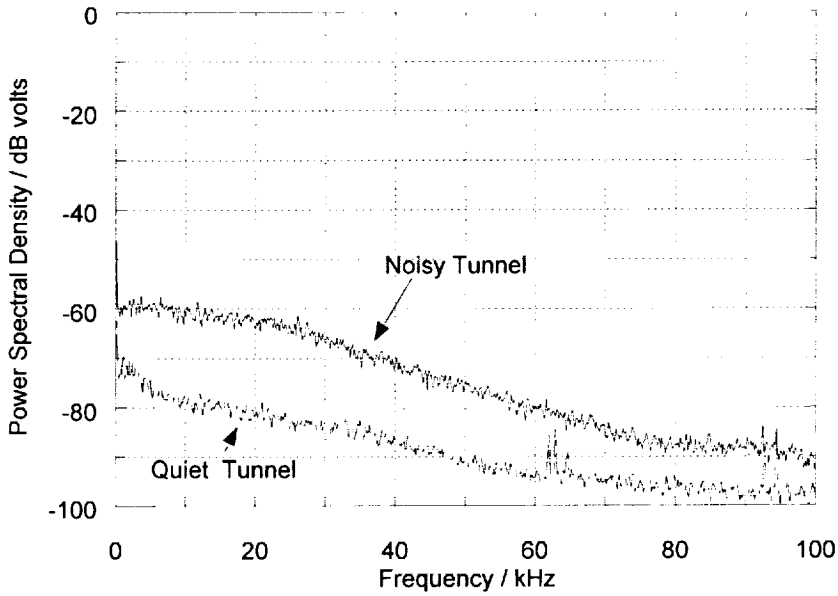

Figure 3. Effect of tripping wind tunnel walls on freestream frequency spectra, tunnel centerline 1.0 inch downstream of the nozzle exit, $Re_\infty = 3.65 \times 10^6$/ft.

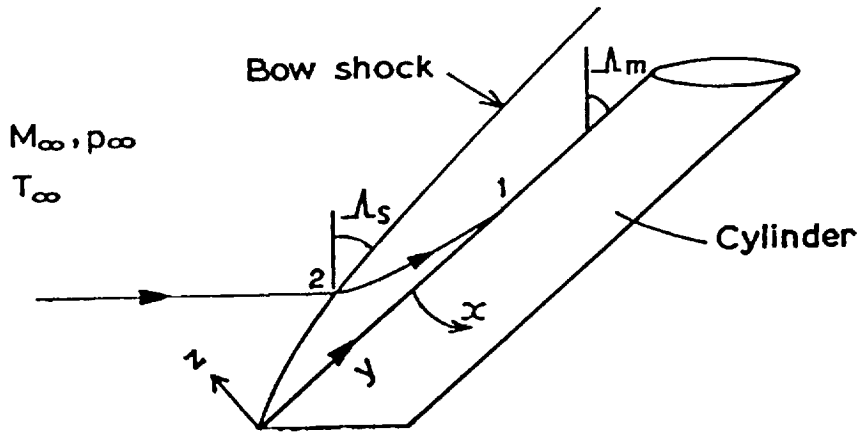

Figure 4. Semi-infinite circular cylinder in supersonic flow.

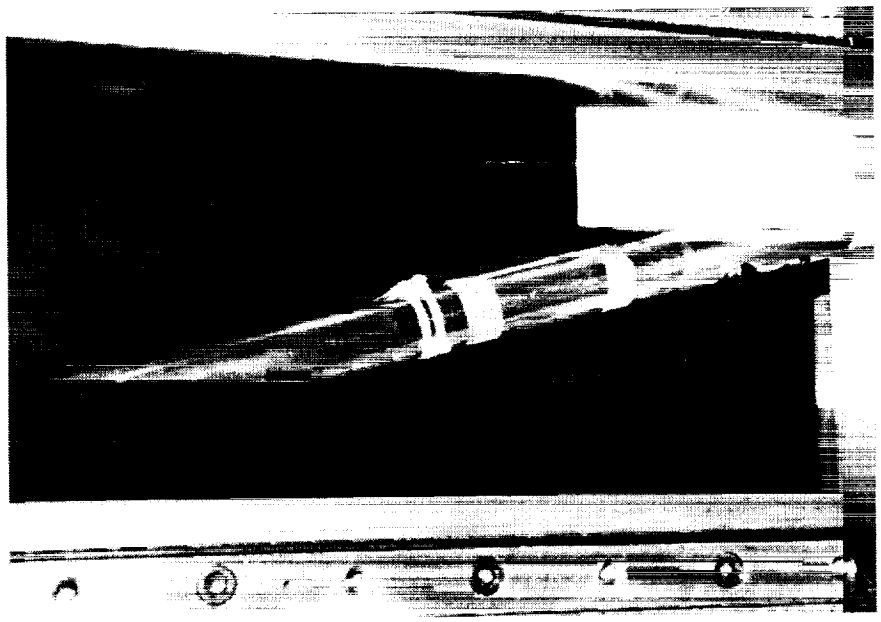

Figure 5. Thermocouple instrumented model set up for trip wire testing.

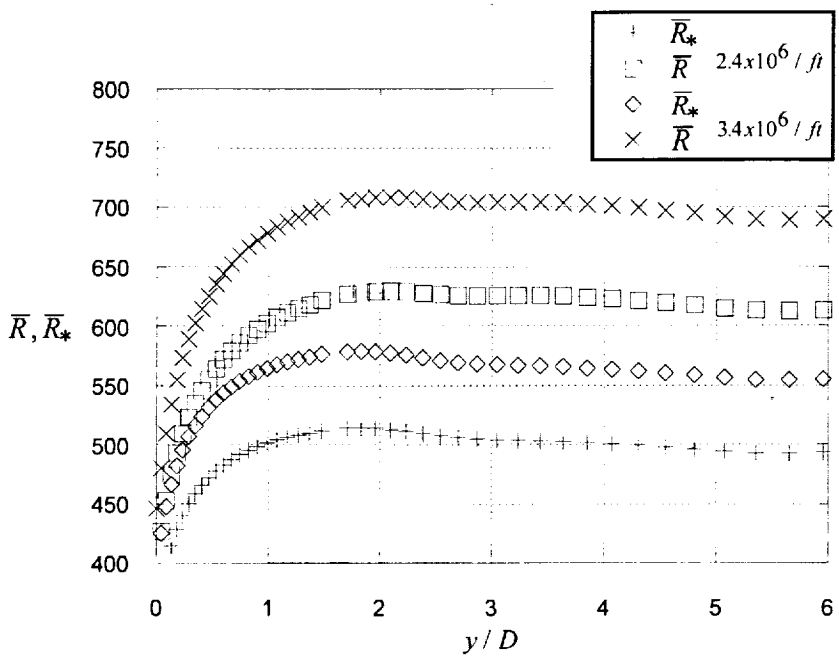

Figure 6. CFD prediction of $\overline{R}$ and $\overline{R}_*$ along the attachment line.

Re_∞ =2. 4x10^6/ft and 3.4x10^6/ft.

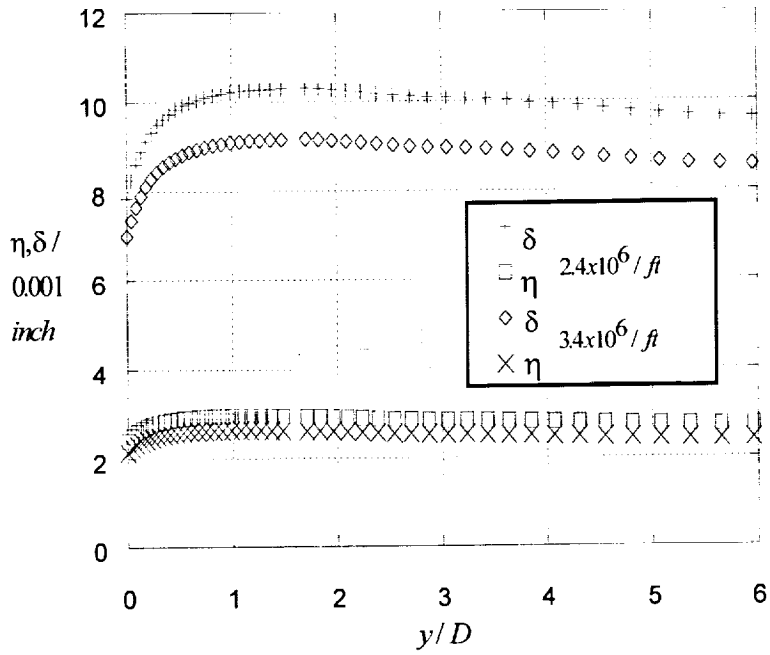

Figure 7. Predicted variation of η and δ along the 76^{o} attachment line.

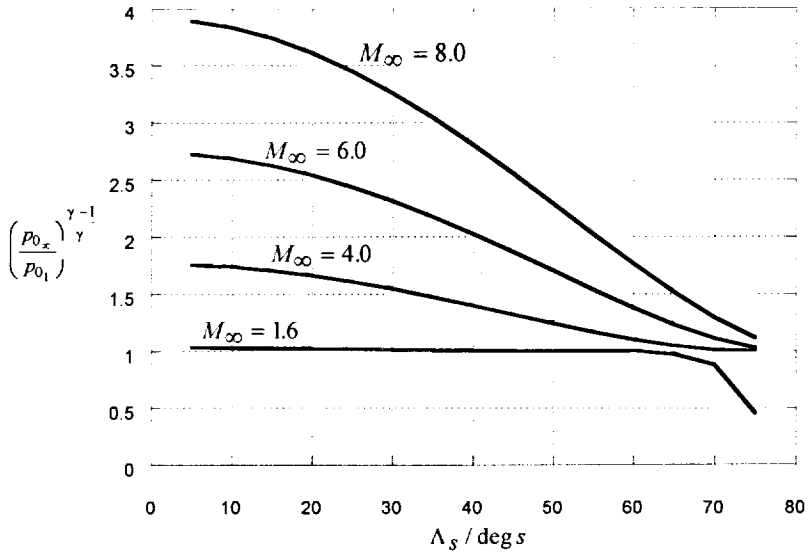

Figure 8. Effect of M_∞ and Λ_s on the total pressure of the streamlines entering the attachment line from the freestream.

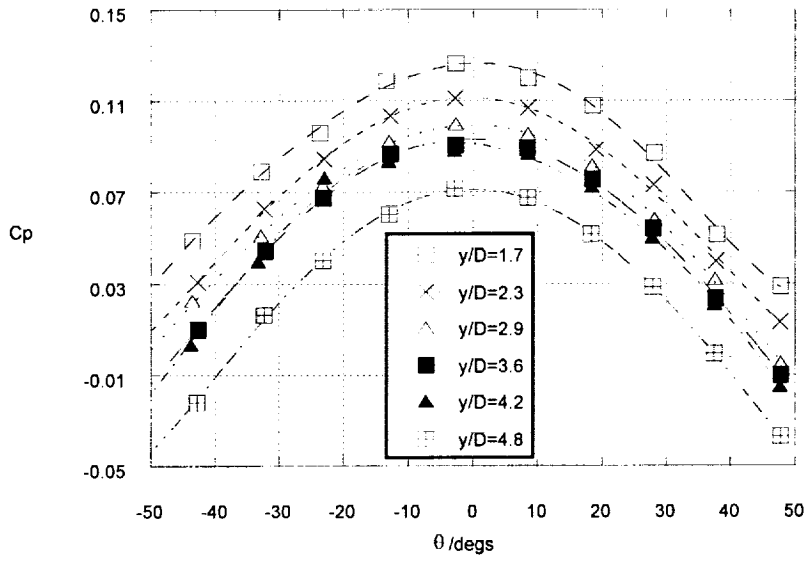

Figure 9. Experimental surface Cp distribution on the swept cylinder.

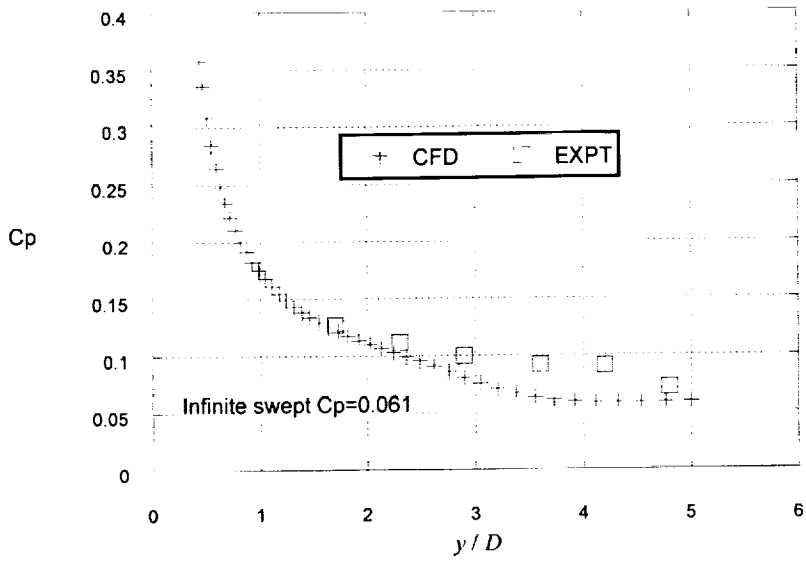

Figure 10. Comparison of the experimental and predicted Cp distributions along the attachment line.

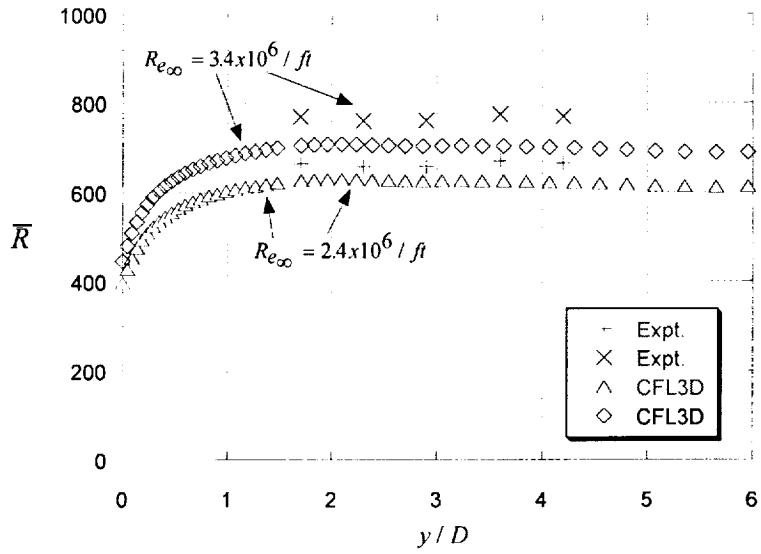

Figure 11. $\overline{R}$ distribution along the attachment line at Re_∞ =2.4x10^6/ft and 3.4x10^6/ft.

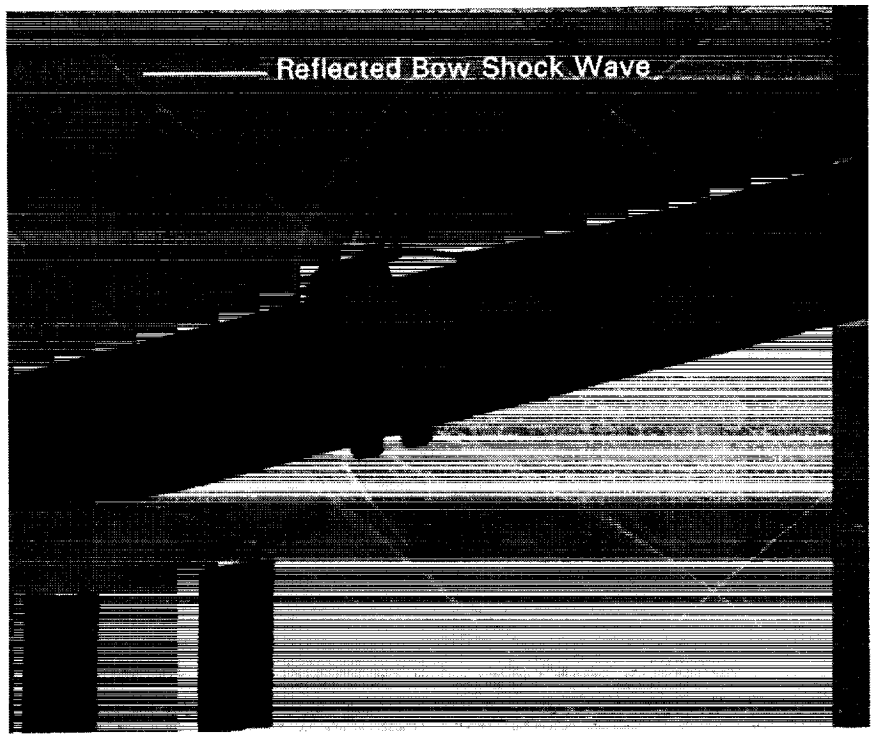

Figure 12. The reflected bow shock wave hits the rear of the hot wire probe body at y/D=5.6.

Re_∞ =2.4x10^6/ft. Distance between tapes is approximately 1 inch.

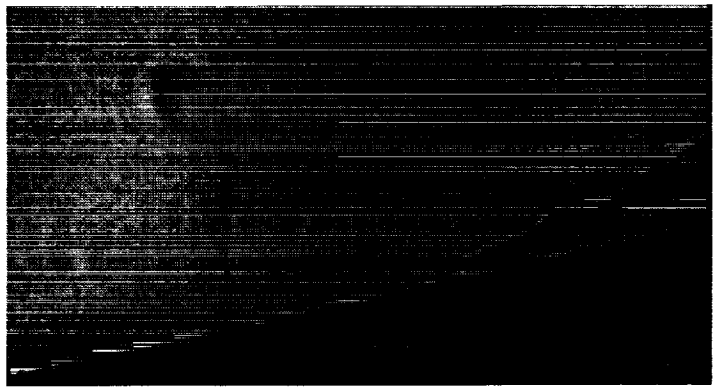

Wind off

Laminar flow. No trip, $\overline{R}$ =790.

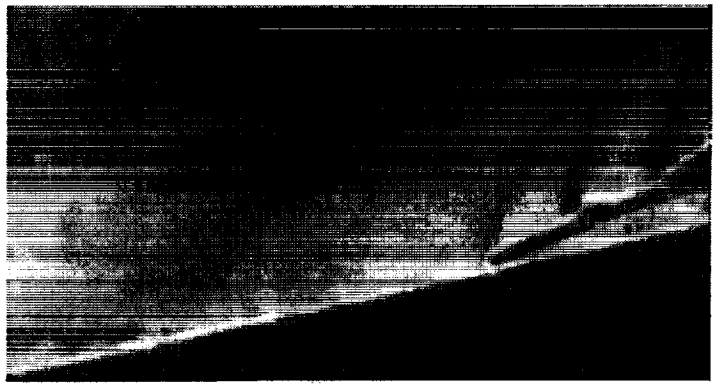

Turbulent flow. 0.025 inch trip wire at y/D=4.2, $\overline{R}$ =790.

Figure 13. Focused Schlieren photographs of the attachment line boundary layer, showing the difference between laminar and turbulent cases. Hot wire at y/D=5.0.

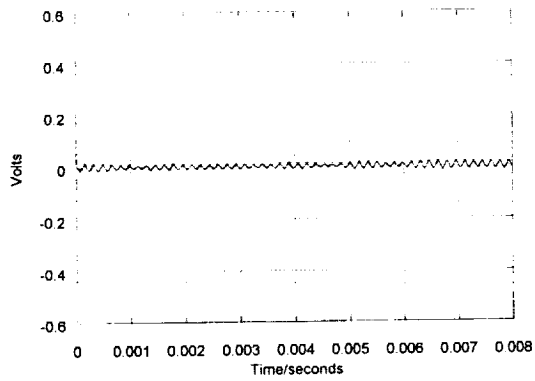

Laminar Flow.

$\overline{R}$ =596 ($\overline{R}_*$ =480), Re_k =1896, k/η =3.10, s/η =517, r=0.864. rms=7mV.

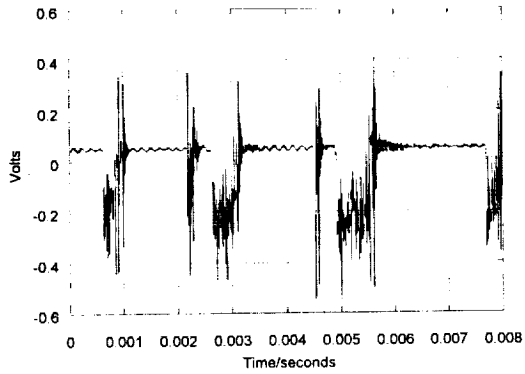

Intermittent Flow (intermittency ≈ 40%).

$\overline{R}$ =657 ($\overline{R}_*$ =529), Re_k =2292, k/η =3.42, s/η =570, r=0.868. rms=121mV.

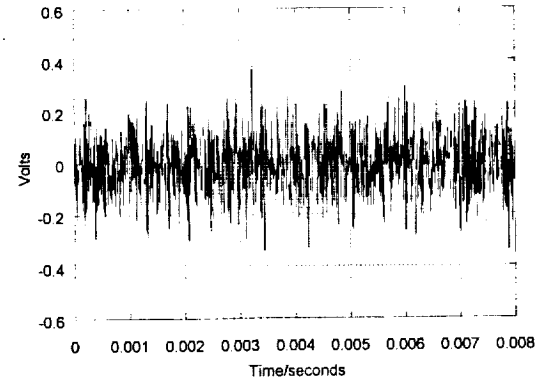

Turbulent Flow (intermittency ≈ 100%).

$\overline{R}$ =700 ($\overline{R}_*$ =560), Re_k =2636, k/η =3.63, s/η =605, r=0.880. rms=98mV.

Figure 14. Observation of laminar, intermittent and turbulent flow with a 0.009 inch Trip Wire at y=6.5 inch (y/D =4.1).

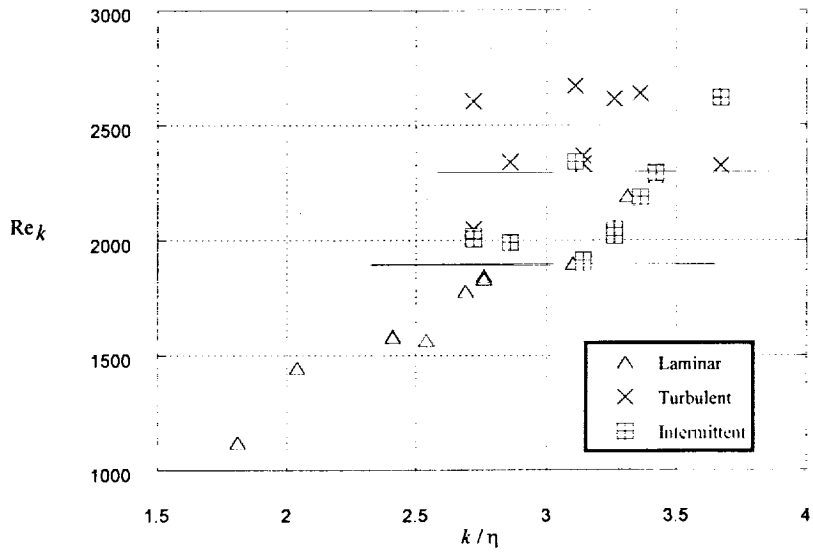

Figure 15. Trip wire Reynolds number as a function of non-dimensional trip height for the onset of transition.

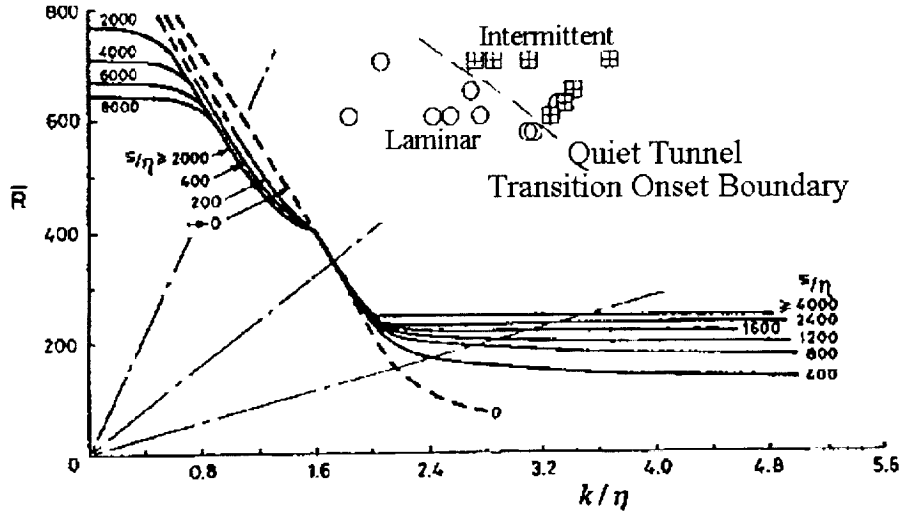

Figure 16. Mach 1.6, low disturbance wind tunnel results compared to correlation of incompressible, attachment-line transition onset with surface roughness height as proposed by Poll.

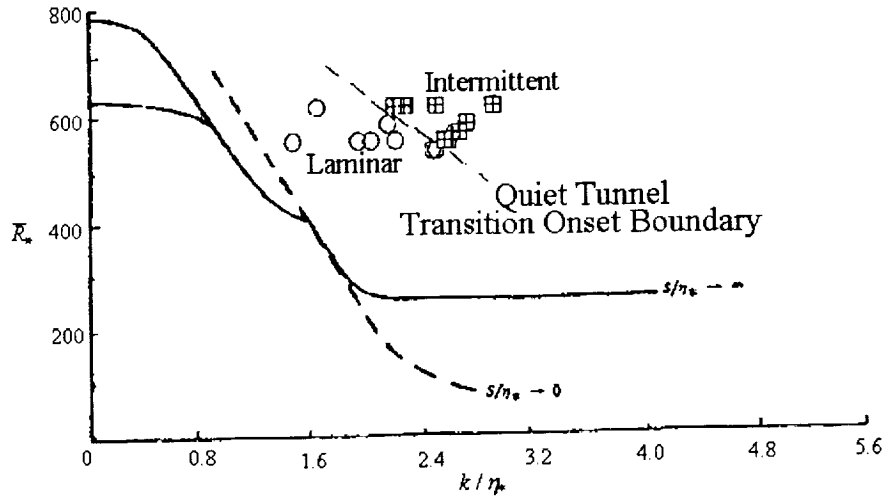

Figure 17. The proposed transformation, based on the reference temperature (Poll), does not completely collapse the present data.